

## Ferromagnetic Mn moments at SrRuO<sub>3</sub>/SrMnO<sub>3</sub> interfaces

Y. Choi<sup>a)</sup>

Materials Science Division, Argonne National Laboratory, Argonne, Illinois 60439

Y. Z. Yoo, O. Chmaissem, A. Ullah, S. Kolesnik, and C. W. Kimball

Institute for NanoScience, Engineering, and Technology, Physics Department, Northern Illinois University, DeKalb, Illinois 60115

D. Haskel

Advanced Photon Source, Argonne National Laboratory, Argonne, Illinois 60439

J. S. Jiang and S. D. Bader

Materials Science Division, Argonne National Laboratory, Argonne, Illinois 60439

(Received 1 May 2007; accepted 5 June 2007; published online 10 July 2007)

Using element-specific, x-ray probes of magnetism the authors observe a net ferromagnetic moment from Mn in SrRuO<sub>3</sub>/SrMnO<sub>3</sub> (SRO/SMO) superlattice films. It is found that the magnetic behavior of the SRO and SMO layers is significantly modified by their exchange interaction. Bulk magnetometry shows a two-step, easy-axis magnetization reversal process and x-ray measurements confirm that the reversal with higher coercivity involves the magnetization in the SMO layers. The results provide strong evidence for the presence of pinned SRO magnetization at the SRO/SMO interface. Angle-dependent measurements reveal that the net Mn moment is due to a canted antiferromagnetic spin configuration in the SMO layers. © 2007 American Institute of Physics.

[DOI: 10.1063/1.2753100]

Magnetic multilayer structures exhibit a myriad of interesting phenomena due to geometrical confinement and physical proximity effects, generating interest from technical and fundamental viewpoints. In magnetic multilayer films, interfacial coupling and finite-size effects can lead to phenomena such as exchange bias and spin flop transitions.<sup>1-4</sup> In strongly correlated, transition metal oxides coupling between orbital and spin degrees of freedom together with interfacial effects can enable potential applications, such as field effect transistors<sup>5</sup> and magnetic tunnel junctions.<sup>6</sup> Perovskite SrRuO<sub>3</sub> (SRO) has received much attention due to its interesting magnetic and electronic properties. SRO is an itinerant ferromagnet ( $T_C \sim 163$  K) whose magnetic and electronic properties can be readily modified by substitution at Sr and/or Ru sites.<sup>7</sup> SrMnO<sub>3</sub> (SMO) is a *G*-type antiferromagnet with perovskite structure and a Néel temperature  $T_N$  of  $\sim 260$  K.<sup>8</sup> Because of a small lattice mismatch, high quality SRO/SMO superlattices can be grown on SrTiO<sub>3</sub> (STO) substrates.<sup>9</sup> In the case of STO (100) substrates, the easy axis of the ferromagnetic SRO layers is in the out-of-plane direction (uniaxial anisotropy near the SRO [110] axis<sup>10</sup>), while the antiferromagnetic SMO layers are expected to have their antiferromagnetically aligned spins in plane.<sup>11</sup> The contact between ferromagnetic and antiferromagnetic layers, together with the relative, orthogonal orientation of anisotropy directions, makes the SRO/SMO system interesting.

The SRO/SMO interface can lead to pinning and biasing properties that significantly influence the magnetization reversal in the superlattices.<sup>12,13</sup> Because of the strong interaction between the SRO and SMO layers at the interfaces, Padhan and Preller proposed that each SRO layer divides into a free internal and two pinned near-interface layers during the magnetization reversal.<sup>12,13</sup> Similarly, the strong in-

terfacial magnetic interactions may also modify the magnetic response of the SMO layers, and it was suggested that the SMO layer contributes to the net in-plane magnetization of the superlattice at higher magnetic field.<sup>12</sup> However, the direct measurement of the magnetic properties of the SMO layers is not trivial because of the dominant magnetic contributions of the SRO layers. Here, we report a magnetization reversal study of the SMO layers using element-specific, x-ray resonant magnetic characterization techniques. These data, in combination with bulk-sensitive superconducting quantum interference device (SQUID) magnetometry data, reveal the response of SMO layers through the reversal of SRO layers. Our results show that the interactions at the interfaces modify the magnetic properties of both the SRO and SMO layers.

Single-crystalline (SRO/SMO)<sub>19</sub> superlattice films were grown on STO (100) substrates by pulsed laser deposition with a KrF excimer laser.<sup>14</sup> Each SRO layer consists of ten unit cells and each SMO layer consists of two unit cells. The superlattices were capped with an extra SRO layer to prevent possible SMO degradation. During growth, the oxygen partial pressure was set at 200 mTorr and the deposition temperature at 760 °C. Typical layer-by-layer growth of alternating SRO and SMO layers was observed and monitored by high-pressure reflection high energy electron diffraction, indicating that the interfaces are of good quality. The temperature dependence of the dc magnetization was measured using SQUID after zero field cooling with an applied field of 0.1 T parallel to the film surface normal (i.e., the magnetic easy axis of the SRO layers). The Curie temperature of our superlattice is close to the bulk value of 163 K.<sup>15,16</sup>

In order to study the magnetic response of the SMO layers, x-ray magnetic circular dichroism (XMCD) and x-ray resonant magnetic scattering (XRMS) measurements were carried out at the Mn  $L_{2,3}$  edges. While the SQUID measurement probes the magnetic response of the whole sample,

<sup>a)</sup>Electronic mail: yschoi@anl.gov

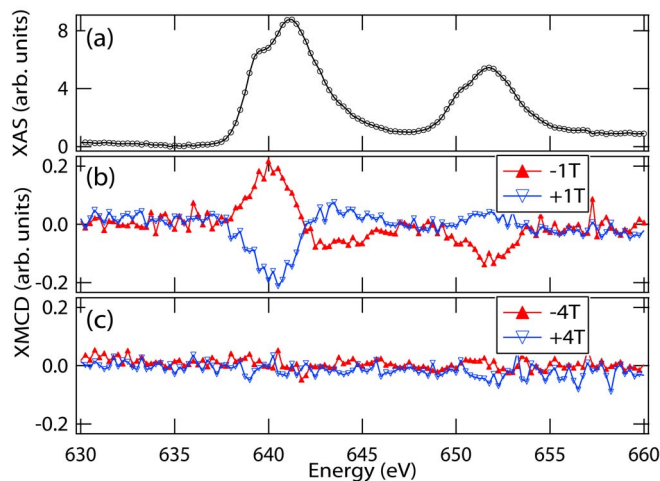


FIG. 1. (Color online) XAS and XMCD data taken at 50 K at the Mn  $L_{2,3}$  edges. The incident x ray and applied field directions were parallel to the film surface normal. XMCD data were taken by reversing the photon helicity at each energy with a fixed field. (a) XAS, (b) XMCD with  $H = \pm 1$  T, and (c) XMCD with  $H = \pm 4$  T.

XMCD and XRMS measurements provide Mn-specific magnetic information. X-ray measurements were performed at beamline 4-ID-C of the Advanced Photon Source at Argonne National Laboratory.<sup>17</sup> X-ray absorption spectra (XAS) and XMCD measured in total electron yield (TEY) and helicity-switching mode near the Mn  $L_{2,3}$  absorption edges are plotted in Fig. 1. Measurements were performed with the magnetic field applied parallel to the x-ray propagation direction, which is along the film normal. With an applied field  $H = \pm 1$  T, significant XMCD signals were measured, as shown in Fig. 1(b). This is unexpected since truly  $G$ -type antiferromagnetic SMO layers should yield no XMCD signal. Since XMCD is proportional to the net magnetic moment of resonant atoms projected along the x-ray propagation direction, our results indicate that the Mn atoms possess a net out-of-plane ferromagnetic moment. However, as the field increases to  $\pm 4$  T, the XMCD signal reduces to zero, as shown in Fig. 1(c). This field dependence suggests either that the net Mn moment disappears or that a net Mn magnetization persists in a direction nearly orthogonal to the  $\pm 4$  T applied field.

We investigated the origin of the observed net Mn moment by comparing the magnetic response of the SMO layers (probed by XMCD) with the response of the whole superlattice (probed by SQUID) at 50 K with a field applied out of plane. As seen in Fig. 2, the SQUID hysteresis loop shows the occurrence of a two-step magnetization reversal process ( $\Delta M1$  and  $\Delta M2$ ). The high field reversal  $\Delta M2$  in the SQUID data has the same coercive field,  $\sim 0.34$  T, as the SMO-specific XMCD data, while the low field reversal  $\Delta M1$  is absent in the XMCD data. This provides unambiguous evidence that the enhanced coercivity of the superlattice relative to that of a single SRO layer (0.15 T at 5 K) is due to the contribution of interfacial regions involving coupling to the net magnetization of SMO layers. We assign the low field reversal  $\Delta M1$  to the switching of free SRO layers (coercive field  $\sim 0.15$  T) and the high field reversal  $\Delta M2$  to the switching of pinned regions at the SRO/SMO interface. We note that the net magnetization in the SMO layer is a small fraction of the total magnetization. This can be seen by saturation of magnetization above  $\sim 0.5$  T as compared to the steep field dependence of the net magnetization in the SMO layers

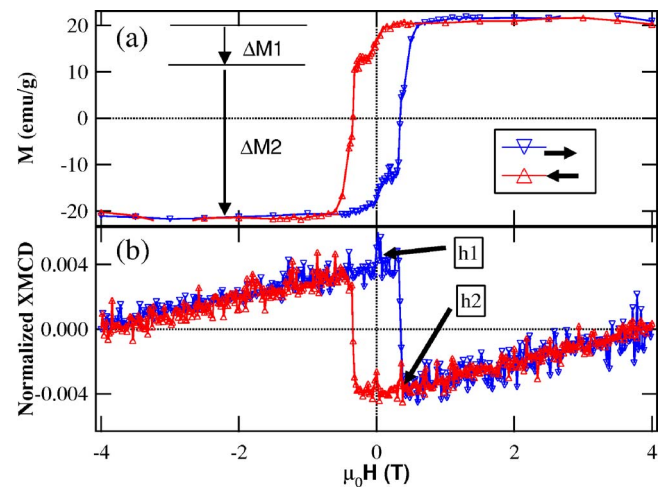


FIG. 2. (Color online) Out-of-plane magnetization measurements at 50 K. (a) Aggregate response from SQUID measurement. (b) Mn-element-specific hysteresis loop from XMCD measurement. The normalized XMCD is defined as  $(I^+ - I^-)/(I^+ + I^-)$ , where  $I^{\pm}$  are the TEYs for the two opposite polarizations of the incoming x rays.

[Fig. 2(b)]. This indicates that the SQUID data are dominated by the SRO layers, as expected, and shows that the higher field reversal process involves a simultaneous reversal of pinned SRO and SMO regions, as a result of the strong coupling at the SRO/SMO interface. A sharp and abrupt reversal of the SMO magnetization is evident in Fig. 2(b), suggesting a sudden change in the Mn spin configuration. To investigate this further, we carried out in-plane, field-dependent SQUID magnetometry and Mn-XRMS measurements,<sup>18,19</sup> as shown in Fig. 3. The net Mn moment increases with the applied field.<sup>20</sup> The in-plane Mn-XRMS loop does not show hysteresis or remanent magnetization, in contrast to the out-of-plane loops of Fig. 2(b). This implies that the in-plane direction, nominally the easy direction for SMO grown on STO (100) substrates, is not the easy axis of the SMO in contact with the SRO layers.

The observed net magnetization in SMO layers that results in nonzero signals in XMCD and XRMS measurements is either due to a ferromagnetic or canted antiferromagnetic arrangement of Mn spins. The out-of-plane Mn-XMCD hysteresis loop in Fig. 2(b) shows a linear suppression of the

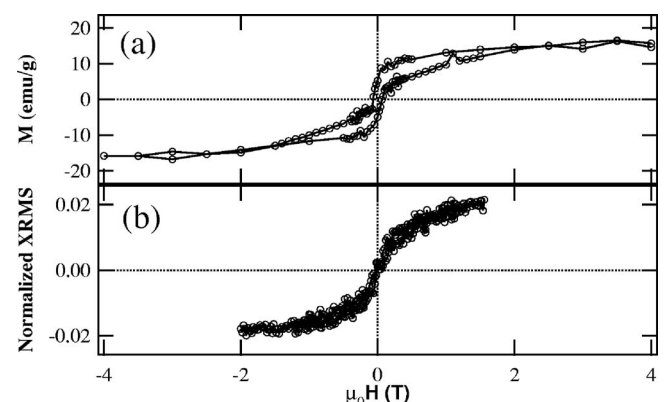


FIG. 3. In-plane magnetization measurements at 50 K. (a) Aggregate response from SQUID measurement. (b) Mn-element-specific hysteresis loop from XRMS measurement. The field direction was at  $10^\circ$  from the film surface plane. The normalized XRMS is defined as  $(I^+ - I^-)/(I^+ + I^-)$ , where  $I^{\pm}$  are the scattered intensities for the two opposite polarizations of the incoming x rays.

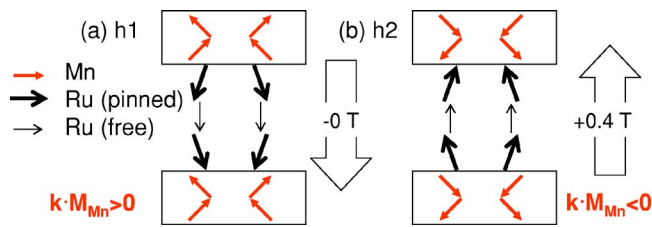


FIG. 4. (Color online) Spin configurations for the fields  $h1$  and  $h2$ , as indicated in Fig. 3(b). The XMCD signal is proportional to  $k \cdot M$ , where  $k$  is the x-ray propagation direction and  $k \parallel H$ .

projected Mn moment as a function of increasing magnetic field. This unexpected behavior indicates that the SMO layers are not likely to be ferromagnetic. In the case of a canted antiferromagnet, one would expect the net projected moment to increase as a function of increasing field if the net moment and the field were aligned in the same direction. However, if the projected Mn moment is antiparallel to the SRO magnetization direction, then the opposite is the case. This latter scenario is consistent with our results and suggests that the exchange coupling between the Ru and Mn moments across the SRO/SMO interfaces is antiferromagnetic, as observed in Mn/Ru superlattices.<sup>21</sup> Cao *et al.* reported that Mn doping changes the SrRuO<sub>3</sub> from being ferromagnetic to antiferromagnetic.<sup>7</sup> Similarly, in SrRu<sub>0.9</sub>Mn<sub>0.1</sub>O<sub>3</sub> polycrystals, it was reported that the Mn–Ru coupling is antiparallel due to hybridization.<sup>22</sup> Antiferromagnetic exchange coupling between two magnetic layers was also found in La<sub>0.67</sub>Sr<sub>0.33</sub>MnO<sub>3</sub>/SrRuO<sub>3</sub> bilayers<sup>23</sup> and in La<sub>0.7</sub>Sr<sub>0.3</sub>MnO<sub>3</sub>/SrRuO<sub>3</sub> superlattices,<sup>24</sup> in agreement with the deduced antiferromagnetic coupling between Ru and Mn across the interfaces in our SRO/SMO system.

Possible spin configurations for two field values  $h1$  and  $h2$  in the out-of-plane hysteresis loops of Fig. 2 are shown schematically in Fig. 4. As the applied field  $H$  is reduced to zero from  $-4$  T, the pinned Ru spins relax, and the Mn spins become canted, as shown in Fig. 4(a), resulting in a nonzero Mn-XMCD signal. As  $H$  becomes increasingly positive, the free Ru spins reverse first, and the pinned Ru spins reverse at a higher field. As the pinned Ru spins reverse, the canted Mn spins reverse simultaneously, leading to the abrupt Mn-XMCD sign reversal of Fig. 2(b) and the spin configuration in Fig. 4(b). As  $H$  keeps increasing positively, a competition between the Zeeman energy and inter/intralayer exchange coupling would determine the rate of reduction in the net Mn moment antiparallel to  $H$ . Our data show that this competition causes the Mn spins to lie close to the in-plane direction. Hence, at high fields, the canting of Mn moments is reduced as the Mn spins lie closer to the in-plane direction, reducing the net Mn moment along the applied field. This causes the linear reduction of Mn-XMCD seen in Fig. 2(b). We note that the configuration in Fig. 4(a) is consistent with the zero remanent magnetization measured in the in-plane XRMS loops [Fig. 3(b)]. The spin configurations in Fig. 4 are consistent with our micromagnetic simulation results. A detailed theoretical work will be presented in a subsequent paper.

The collective magnetic behavior of the dissimilar SRO and SMO layers is significantly modified due to their proximity. Using conventional and Mn-specific probes of magnetization, we observed an interesting field dependence in our SRO/SMO superlattice. A comparative study of the two probes shows clear evidence of pinned SRO layers near the interfaces and provides evidence of canting of the Mn spins in the SMO layers as a result of the competition between anisotropy and antiferromagnetic exchange coupling interactions at the SRO/SMO interface.

Work at NIU was supported by the Institute for Nano-Science, Engineering and Technology, U.S. Department of Education. Work at Argonne National Laboratory was supported by U.S. Department of Energy, Office of Science, under Contract No. DE-AC02-06CH11357.

- <sup>1</sup>W. H. Meiklejohn and C. P. Bean, *Phys. Rev.* **102**, 1413 (1956).
- <sup>2</sup>J. Nogus and I. K. Schuller, *J. Magn. Magn. Mater.* **192**, 203 (1999).
- <sup>3</sup>A. E. Berkowitz and K. Takano, *J. Magn. Magn. Mater.* **200**, 552 (1999).
- <sup>4</sup>S. G. E. teVelthuis, J. S. Jiang, S. D. Bader, and G. P. Felcher, *Phys. Rev. Lett.* **89**, 127203 (2002).
- <sup>5</sup>C. H. Ahn, S. Gariglio, P. Paruch, T. Tybell, L. Antognazza, and J.-M. Triscone, *Science* **284**, 1152 (1999).
- <sup>6</sup>H. Yamada, Y. Ogawa, Y. Ishii, H. Sato, H. Akoh, M. Kawasaki, and Y. Tokura, *Science* **305**, 646 (2004).
- <sup>7</sup>G. Cao, S. Chikara, X. N. Lin, E. Elhami, V. Durairaj, and P. Schlottmann, *Phys. Rev. B* **71**, 035104 (2005).
- <sup>8</sup>T. Takeda and S. Ohara, *J. Phys. Soc. Jpn.* **37**, 275 (1974); O. Chmaissem, B. Dabrowski, S. Kolesnik, J. Mais, D. E. Brown, R. Kruk, P. Prior, B. Pyles, and J. D. Jorgensen, *Phys. Rev. B* **64**, 134412 (2001).
- <sup>9</sup>P. Padhan, W. Prellier, and B. Mercey, *Phys. Rev. B* **70**, 184419 (2004).
- <sup>10</sup>Y. Z. Yoo, O. Chmaissem, S. Kolesnik, A. Ullah, L. B. Lurio, D. E. Brown, J. Brady, B. Dabrowski, C. W. Kimball, M. Haji-Sheikh, and A. P. Genis, *Appl. Phys. Lett.* **89**, 124104 (2006).
- <sup>11</sup>Bulk SMO has a cubic structure with a  $G$ -type antiferromagnetic spin arrangement. However, SMO films on SrTiO<sub>3</sub> (100) substrates are most likely to have in-plane antiferromagnetic spin alignment due to in-plane lattice elongation and out-of-plane lattice compression.
- <sup>12</sup>P. Padhan and W. Prellier, *Phys. Rev. B* **72**, 104416 (2005).
- <sup>13</sup>P. Padhan and W. Prellier, *Appl. Phys. Lett.* **88**, 263114 (2006).
- <sup>14</sup>Y. Z. Yoo, O. Chmaissem, S. Kolesnik, B. Dabrowski, M. Maxwell, C. W. Kimball, L. McAnelly, M. Haji-Sheikh, and A. P. Genis, *J. Appl. Phys.* **97**, 103525 (2005).
- <sup>15</sup>A. Callaghan, C. W. Moeller, and R. Ward, *Inorg. Chem.* **5**, 1572 (1966).
- <sup>16</sup>A. Kanbayasi, *J. Phys. Soc. Jpn.* **41**, 1876 (1976).
- <sup>17</sup>J. W. Freeland, J. C. Lang, G. Srajer, R. Winarski, D. Shu, and D. M. Mills, *Rev. Sci. Instrum.* **73**, 1408 (2001).
- <sup>18</sup>C. Kao, J. B. Hastings, E. D. Johnson, D. P. Siddons, G. C. Smith, and G. A. Prinz, *Phys. Rev. Lett.* **65**, 373 (1990); J. W. Freeland, K. Busmann, P. Lubitz, Y. U. Idzerda, and C.-C. Kao, *Appl. Phys. Lett.* **73**, 2206 (1998).
- <sup>19</sup>At low x-ray incident angles, TEY signals were too small so that the scattered intensities were used to measure the field dependence of the Mn moment.
- <sup>20</sup>We note that the magnitude of XRMS and XMCD signals cannot be directly compared because the former is affected by charge scattering.
- <sup>21</sup>V. Dupuis, M. Maurer, M. Piecuch, M. F. Ravet, J. Dekoster, S. Andrieu, J. F. Bobo, F. Baudelet, P. Bauer, and A. Fontaine, *Phys. Rev. B* **48**, 5585 (1993).
- <sup>22</sup>Z. H. Han, J. I. Budnick, W. A. Hines, B. Dabrowski, and T. Maxwell, *Appl. Phys. Lett.* **89**, 102501 (2006).
- <sup>23</sup>X. Ke, M. S. Rzchowski, L. J. Belenky, and C. B. Eom, *Appl. Phys. Lett.* **84**, 5458 (2004).
- <sup>24</sup>P. Padhan, W. Prellier, and R. C. Budhani, *Appl. Phys. Lett.* **88**, 192509 (2006).